

¹ **Critical transitions and the fragmenting of global forests**

² **Leonardo A. Saravia^{1 3}, Santiago R. Doyle¹, Benjamin Bond-Lamberty²**

³ 1. Instituto de Ciencias, Universidad Nacional de General Sarmiento, J.M. Gutierrez 1159 (1613), Los
⁴ Polvorines, Buenos Aires, Argentina.

⁵ 2. Pacific Northwest National Laboratory, Joint Global Change Research Institute at the University of
⁶ Maryland–College Park, 5825 University Research Court #3500, College Park, MD 20740, USA

⁷ 3. Corresponding author e-mail: lsaravia@ungs.edu.ar

⁸ **Keywords:** Forest fragmentation, early warning signals, percolation, power-laws, MODIS, critical transitions

⁹ **Running title:** Critical fragmentation in global forest

¹⁰ **Abstract**

¹¹ 1. Forests provide critical habitat for many species, essential ecosystem services, and are coupled to
¹² atmospheric dynamics through exchanges of energy, water and gases. One of the most important
¹³ changes produced in the biosphere is the replacement of forest areas with human dominated landscapes.
¹⁴ This usually leads to fragmentation, altering the sizes of patches, the structure and function of the
¹⁵ forest. Here we studied the distribution and dynamics of forest patch sizes at a global level, examining
¹⁶ signals of a critical transition from an unfragmented to a fragmented state.

¹⁷ 2. We used MODIS vegetation continuous field to estimate the forest patches at a global level and de-
¹⁸ fined wide regions of connected forest across continents and big islands. We search for critical phase
¹⁹ transitions, where the system state of the forest changes suddenly at a critical point in time; this
²⁰ implies an abrupt change in connectivity that causes an increased fragmentation level. We studied the
²¹ distribution of forest patch sizes and the dynamics of the largest patch over the last fourteen years,
²² as the conditions that indicate that a region is near a critical fragmentation threshold are related to
²³ patch size distribution and temporal fluctuations of the largest patch.

²⁴ 3. We found some evidence that allows us to analyze fragmentation as a critical transition: most regions
²⁵ followed a power-law distribution over the 14 years. We also found that the Philippines region probably
²⁶ went through a critical transition from a fragmented to an unfragmented state. Only the tropical forest
²⁷ of Africa and South America met the criteria to be near a critical fragmentation threshold.

²⁸ 4. This implies that human pressures and climate forcings might trigger undesired effects of fragmentation,

29 such as species loss and degradation of ecosystems services, in these regions. The simple criteria
30 proposed here could be used as an early warning to estimate the distance to a fragmentation threshold
31 in forest around the globe and a predictor of a planetary tipping point.

32 Introduction

33 Forests are one of the most important biomes on earth, providing habitat for a large proportion of species
34 and contributing extensively to global biodiversity (Crowther *et al.* 2015). In the previous century human
35 activities have influenced global bio-geochemical cycles (Bonan 2008; Canfield, Glazer & Falkowski 2010),
36 with one of the most dramatic changes being the replacement of 40% of Earth's formerly biodiverse land
37 areas with landscapes that contain only a few species of crop plants, domestic animals and humans (Foley
38 *et al.* 2011). These local changes have accumulated over time and now constitute a global forcing (Barnosky
39 *et al.* 2012).

40 Another global scale forcing that is tied to habitat destruction is fragmentation, which is defined as the
41 division of a continuous habitat into separated portions that are smaller and more isolated. Fragmentation
42 produces multiple interwoven effects: reductions of biodiversity between 13% and 75%, decreasing forest
43 biomass, and changes in nutrient cycling (Haddad *et al.* 2015). The effects of fragmentation are not only
44 important from an ecological point of view but also that of human activities, as ecosystem services are deeply
45 influenced by the level of landscape fragmentation (Mitchell *et al.* 2015).

46 Ecosystems have complex interactions between species and present feedbacks at different levels of organization
47 (Gilman *et al.* 2010), and external forcings can produce abrupt changes from one state to another, called
48 critical transitions (Scheffer *et al.* 2009). These abrupt state shifts cannot be linearly forecasted from past
49 changes, and are thus difficult to predict and manage (Scheffer *et al.* 2009). Such 'critical' transitions have
50 been detected mostly at local scales (Drake & Griffen 2010; Carpenter *et al.* 2011), but the accumulation of
51 changes in local communities that overlap geographically can propagate and theoretically cause an abrupt
52 change of the entire system at larger scales (Barnosky *et al.* 2012). Coupled with the existence of global
53 scale forcings, this implies the possibility that a critical transition could occur at a global scale (Rockstrom
54 *et al.* 2009; Folke *et al.* 2011).

55 Complex systems can experience two general classes of critical transitions (Solé 2011). In so-called first
56 order transitions, a catastrophic regime shift that is mostly irreversible occurs because of the existence of
57 alternative stable states (Scheffer *et al.* 2001). This class of transitions is suspected to be present in a variety
58 of ecosystems such as lakes, woodlands, coral reefs (Scheffer *et al.* 2001), semi-arid grasslands (Bestelmeyer
59 *et al.* 2011), and fish populations (Vasilakopoulos & Marshall 2015). They can be the result of positive
60 feedback mechanisms (Martín *et al.* 2015); for example, fires in some forest ecosystems were more likely to
61 occur in previously burned areas than in unburned places (Kitzberger *et al.* 2012).

62 The other class of critical transitions are continuous or second order transitions (Solé & Bascompte 2006).

63 In these cases, there is a narrow region where the system suddenly changes from one domain to another,
64 with the change being continuous and in theory reversible. This kind of transitions were suggested to be
65 present in tropical forest (Pueyo *et al.* 2010), semi-arid mountain ecosystems (McKenzie & Kennedy 2012),
66 tundra shrublands (Naito & Cairns 2015). The transition happens at a critical point where we can observe a
67 distinctive spatial pattern: scale invariant fractal structures characterized by power law patch distributions
68 (Stauffer & Aharony 1994).

69 There are several processes that can convert a catastrophic transition to a second order transitions (Martín
70 *et al.* 2015). These include stochasticity, such as demographic fluctuations, spatial heterogeneities, and/or
71 dispersal limitation. All these components are present in forest around the globe (Seidler & Plotkin 2006;
72 Filotas *et al.* 2014; Fung *et al.* 2016), and thus continuous transitions might be more probable than
73 catastrophic transitions. Moreover there is some evidence of recovery in some systems that supposedly
74 suffered an irreversible transition produced by overgrazing (Zhang *et al.* 2005) and desertification (Allington
75 & Valone 2010).

76 The spatial phenomena observed in continuous critical transitions deal with connectivity, a fundamental
77 property of general systems and ecosystems from forests (Ochoa-Quintero *et al.* 2015) to marine ecosystems
78 (Leibold & Norberg 2004) and the whole biosphere (Lenton & Williams 2013). When a system goes from a
79 fragmented to a connected state we say that it percolates (Solé 2011). Percolation implies that there is a
80 path of connections that involves the whole system. Thus we can characterize two domains or phases: one
81 dominated by short-range interactions where information cannot spread, and another in which long range
82 interactions are possible and information can spread over the whole area. (The term “information” is used
83 in a broad sense and can represent species dispersal or movement.)

84 Thus, there is a critical “percolation threshold” between the two phases, and the system could be driven
85 close to or beyond this point by an external force; climate change and deforestation are the main forces
86 that could be the drivers of such a phase change in contemporary forests (Bonan 2008; Haddad *et al.* 2015).
87 There are several applications of this concept in ecology: species’ dispersal strategies are influenced by
88 percolation thresholds in three-dimensional forest structure (Solé, Bartumeus & Gamarra 2005), and it has
89 been shown that species distributions also have percolation thresholds (He & Hubbell 2003). This implies
90 that pushing the system below the percolation threshold could produce a biodiversity collapse (Bascompte
91 & Solé 1996; Solé, Alonso & Saldaña 2004; Pardini *et al.* 2010); conversely, being in a connected state (above
92 the threshold) could accelerate the invasion of forest into prairie (Loehle, Li & Sundell 1996; Naito & Cairns
93 2015).

94 One of the main challenges with systems that can experience critical transitions—of any kind—is that the

95 value of the critical threshold is not known in advance. In addition, because near the critical point a small
96 change can precipitate a state shift of the system, they are difficult to predict. Several methods have been
97 developed to detect if a system is close to the critical point, e.g. a deceleration in recovery from perturbations,
98 or an increase in variance in the spatial or temporal pattern (Hastings & Wysham 2010; Carpenter *et al.*
99 2011; Boettiger & Hastings 2012; Dai *et al.* 2012).

100 In this study, our objective is to look for evidence that forests around the globe are near continuous critical
101 point that represent a fragmentation threshold. We use the framework of percolation to first evaluate if
102 forest patch distribution at a continental scale is described by a power law distribution and then examine
103 the fluctuations of the largest patch. The advantage of using data at a continental scale is that for very large
104 systems the transitions are very sharp (Solé 2011) and thus much easier to detect than at smaller scales,
105 where noise can mask the signals of the transition.

106 Methods

107 Study areas definition

108 We analyzed mainland forests at a continental scale, covering the whole globe, by delimiting land areas with
109 a near-contiguous forest cover, separated with each other by large non-forested areas. Using this criterion,
110 we delimited the following forest regions. In America, three regions were defined: South America temperate
111 forest (SAT), subtropical and tropical forest up to Mexico (SAST), and USA and Canada forest (NA). Europe
112 and North Asia were treated as one region (EUAS). The rest of the delimited regions were South-east Asia
113 (SEAS), Africa (AF), and Australia (OC). We also included in the analysis islands larger than 10^5 km². The
114 mainland region has the number 1 e.g. OC1, and the nearby islands have consecutive numeration (Appendix
115 S4, figure S1-S6).

116 Forest patch distribution

117 We studied forest patch distribution in each defined area from 2000 to 2014 using the MODerate-resolution
118 Imaging Spectroradiometer (MODIS) Vegetation Continuous Fields (VCF) Tree Cover dataset version 051
119 (DiMiceli *et al.* 2015). This dataset is produced at a global level with a 231-m resolution, from 2000 onwards
120 on an annual basis. There are several definition of forest based on percent tree cover (Sexton *et al.* 2015);
121 we choose a 30% threshold to convert the percentage tree cover to a binary image of forest and non-forest
122 pixels. This was the definition used by the United Nations' International Geosphere-Biosphere Programme
123 (Belward 1996), and studies of global fragmentation (Haddad *et al.* 2015). This definition avoids the errors

124 produced by low discrimination of MODIS VCF between forest and dense herbaceous vegetation at low forest
125 cover (Sexton *et al.* 2015). Patches of contiguous forest were determined in the binary image by grouping
126 connected forest pixels using a neighborhood of 8 forest units (Moore neighborhood).

127 **Percolation theory**

128 A more in-depth introduction to percolation theory can be found elsewhere (Stauffer & Aharony 1994) and
129 a review from an ecological point of view is available (Oborny, Szabó & Meszéna 2007). Here, to explain
130 the basic elements of percolation theory we formulate a simple model: we represent our area of interest by a
131 square lattice and each site of the lattice can be occupied—e.g. by forest—with a probability p . The lattice
132 will be more occupied when p is greater, but the sites are randomly distributed. We are interested in the
133 connection between sites, so we define a neighborhood as the eight adjacent sites surrounding any particular
134 site. The sites that are neighbors of other occupied sites define a patch. When there is a patch that connects
135 the lattice from opposite sides, it is said that the system percolates. When p is increased from low values, a
136 percolating patch suddenly appears at some value of p called the critical point p_c .

137 Thus percolation is characterized by two well defined phases: the unconnected phase when $p < p_c$ (called
138 subcritical in physics), in which species cannot travel far inside the forest, as it is fragmented; in a general
139 sense, information cannot spread. The second is the connected phase when $p > p_c$ (supercritical), species
140 can move inside a forest patch from side to side of the area (lattice), i.e. information can spread over the
141 whole area. Near the critical point several scaling laws arise: the structure of the patch that spans the area
142 is fractal, the size distribution of the patches is power-law, and other quantities also follow power-law scaling
143 (Stauffer & Aharony 1994).

144 The value of the critical point p_c depends on the geometry of the lattice and on the definition of the
145 neighborhood, but other power-law exponents only depend on the lattice dimension. Close to the critical
146 point, the distribution of patch sizes is:

147 (1) $n_s(p_c) \propto s^{-\alpha}$

148 where $n_s(p)$ is the number of patches of size s . The exponent α does not depend on the details of the
149 model and it is called universal (Stauffer & Aharony 1994). These scaling laws can be applied for landscape
150 structures that are approximately random, or at least only correlated over short distances (Gastner *et al.*
151 2009). In physics this is called “isotropic percolation universality class”, and corresponds to an exponent
152 $\alpha = 2.05495$. If we observe that the patch size distribution has another exponent it will not belong to this
153 universality class and some other mechanism should be invoked to explain it. Percolation thresholds can also

154 be generated by models that have some kind of memory (Hinrichsen 2000; Ódor 2004): for example, a patch
155 that has been exploited for many years will recover differently than a recently deforested forest patch. In
156 this case, the system could belong to a different universality class, or in some cases there is no universality,
157 in which case the value of α will depend on the parameters and details of the model (Corrado, Cherubini &
158 Pennetta 2014).

159 To illustrate these concepts, we conducted simulations with a simple forest model with only two states: forest
160 and non-forest. This type of model is called a “contact process” and was introduced for epidemics (Harris
161 1974), but has many applications in ecology (Solé & Bascompte 2006; Gastner *et al.* 2009). A site with forest
162 can become extinct with probability e , and produce another forest site in a neighborhood with probability
163 c . We use a neighborhood defined by an isotropic power law probability distribution. We defined a single
164 control parameter as $\lambda = c/e$ and ran simulations for the subcritical fragmentation state $\lambda < \lambda_c$, with $\lambda = 2$,
165 near the critical point for $\lambda = 2.5$, and for the supercritical state with $\lambda = 5$ (see supplementary data, gif
166 animations).

167 Patch size distributions

168 We fitted the empirical distribution of forest patch areas, based on the MODIS-derived data described above,
169 to four distributions using maximum likelihood estimation (Goldstein, Morris & Yen 2004; Clauset, Shalizi
170 & Newman 2009). The distributions were: power-law, power-law with exponential cut-off, log-normal, and
171 exponential. We assumed that the patch size distribution is a continuous variable that was discretized by
172 remote sensing data acquisition procedure.

173 We set a minimal patch size (X_{min}) at nine pixels to fit the patch size distributions to avoid artifacts at patch
174 edges due to discretization (Weerman *et al.* 2012). Besides this hard X_{min} limit we set due to discretization,
175 the power-law distribution needs a lower bound for its scaling behavior. This lower bound is also estimated
176 from the data by maximizing the Kolmogorov-Smirnov (KS) statistic, computed by comparing the empirical
177 and fitted cumulative distribution functions (Clauset *et al.* 2009). We also calculated the uncertainty of the
178 parameters using a non-parametric bootstrap method (Efron & Tibshirani 1994), and computed corrected
179 Akaike Information Criteria (AIC_c) and Akaike weights for each model (Burnham & Anderson 2002). Akaike
180 weights (w_i) are the weight of evidence in favor of model i being the actual best model given that one of the
181 N models must be the best model for that set of N models.

182 Additionally, we computed the goodness of fit of the power-law model following the bootstrap approach
183 described by Clauset et. al (2009), where simulated data sets following the fitted model are generated, and a

184 p -value computed as the proportion of simulated data sets that has a KS statistic less extreme than empirical
185 data. The criterion to reject the power law model suggested by Clauset et. al (2009) was $p \leq 0.1$, but as we
186 have a very large n , meaning that negligible small deviations could produce a rejection (Klaus, Yu & Plenz
187 2011), we chose a $p \leq 0.05$ to reject the power law model.

188 To test for differences between the fitted power law exponent for each study area we used a generalized least
189 squares linear model (Zuur *et al.* 2009) with weights and a residual auto-correlation structure. Weights were
190 the bootstrapped 95% confidence intervals and we added an auto-regressive model of order 1 to the residuals
191 to account for temporal autocorrelation.

192 Largest patch dynamics

193 The largest patch is the one that connects the highest number of sites in the area. This has been used
194 extensively to indicate fragmentation (Gardner & Urban 2007; Ochoa-Quintero *et al.* 2015). The relation of
195 the size of the largest patch S_{max} to critical transitions has been extensively studied in relation to percolation
196 phenomena (Stauffer & Aharony 1994; Bazant 2000; Botet & Ploszajczak 2004), but seldom used in ecological
197 studies (for an exception see Gastner *et al.* (2009)). When the system is in a connected state ($p > p_c$) the
198 landscape is almost insensitive to the loss of a small fraction of forest, but close to the critical point a minor
199 loss can have important effects (Solé & Bascompte 2006; Oborny *et al.* 2007), because at this point the
200 largest patch will have a filamentary structure, i.e. extended forest areas will be connected by thin threads.
201 Small losses can thus produce large fluctuations.

202 One way to evaluate the fragmentation of the forest is to calculate the proportion of the largest patch against
203 the total area (Keitt, Urban & Milne 1997). The total area of the regions we are considering (Appendix S4,
204 figures S1-S6) may not be the same than the total area that the forest could potentially occupy, thus a more
205 accurate way to evaluate the weight of S_{max} is to use the total forest area, that can be easily calculated
206 summing all the forest pixels. We calculate the proportion of the largest patch for each year, dividing S_{max}
207 by the total forest area of the same year: $RS_{max} = S_{max}/\sum_i S_i$. This has the effect of reducing the S_{max}
208 fluctuations produced due to environmental or climatic changes influences in total forest area. When the
209 proportion RS_{max} is large (more than 60%) the largest patch contains most of the forest so there are fewer
210 small forest patches and the system is probably in a connected phase. Conversely, when it is low (less than
211 20%), the system is probably in a fragmented phase (Saravia & Momo 2017).

212 The RS_{max} is a useful qualitative index that does not tell us if the system is near or far from the critical
213 transition; this can be evaluated using the temporal fluctuations. We calculate the fluctuations around the

214 mean with the absolute values $\Delta S_{max} = S_{max}(t) - \langle S_{max} \rangle$, using the proportions of RS_{max} . To characterize
215 fluctuations we fitted three empirical distributions: power-law, log-normal, and exponential, using the same
216 methods described previously. We expect that large fluctuation near a critical point have heavy tails (log-
217 normal or power-law) and that fluctuations far from a critical point have exponential tails, corresponding
218 to Gaussian processes (Rooij *et al.* 2013). As the data set spans 15 years, we do not have enough power to
219 reliably detect which distribution is better (Clauset *et al.* 2009). To improve this we performed the goodness
220 of fit test described above for all the distributions. We generated animated maps showing the fluctuations
221 of the two largest patches to aid in the interpretations of the results.

222 A robust way to detect if the system is near a critical transition is to analyze the increase in variance of
223 the density (Benedetti-Cecchi *et al.* 2015). It has been demonstrated that the variance increase in density
224 appears when the system is very close to the transition (Corrado *et al.* 2014), thus practically it does
225 not constitute an early warning indicator. An alternative is to analyze the variance of the fluctuations of
226 the largest patch ΔS_{max} : the maximum is attained at the critical point but a significant increase occurs
227 well before the system reaches the critical point (Corrado *et al.* 2014). In addition, before the critical
228 fragmentation, the skewness of the distribution of ΔS_{max} should be negative, implying that fluctuations
229 below the average are more frequent. We characterized the increase in the variance using quantile regression:
230 if variance is increasing the slopes of upper or/and lower quartiles should be positive or negative.

231 All statistical analyses were performed using the GNU R version 3.3.0 (R Core Team 2015), using code
232 provided by Cosma R. Shalizi for fitting the power law with exponential cutoff model and the poweRlaw
233 package (Gillespie 2015) for fitting the other distributions. For the generalized least squares linear model we
234 used the R function gls from package nlme (Pinheiro *et al.* 2016); and we fitted quantile regressions using
235 the R package quantreg (Koenker 2016). Image processing was done in MATLAB r2015b (The Mathworks
236 Inc.). The complete source code for image processing and statistical analysis, and the patch size data files
237 are available at figshare <http://dx.doi.org/10.6084/m9.figshare.4263905>.

238 Results

239 The figure 1 shows an example of the distribution of the biggest 200 patches for years 2000 and 2014, this
240 distribution is highly variable, but the biggest patch usually maintains its place. Sometimes the biggest
241 patch breaks and then big fluctuations in its size are observed, as we will analyze below. Smaller patches
242 can merge or break more easily so they enter or leave the list of 200, and this is why there is a color change
243 across years.

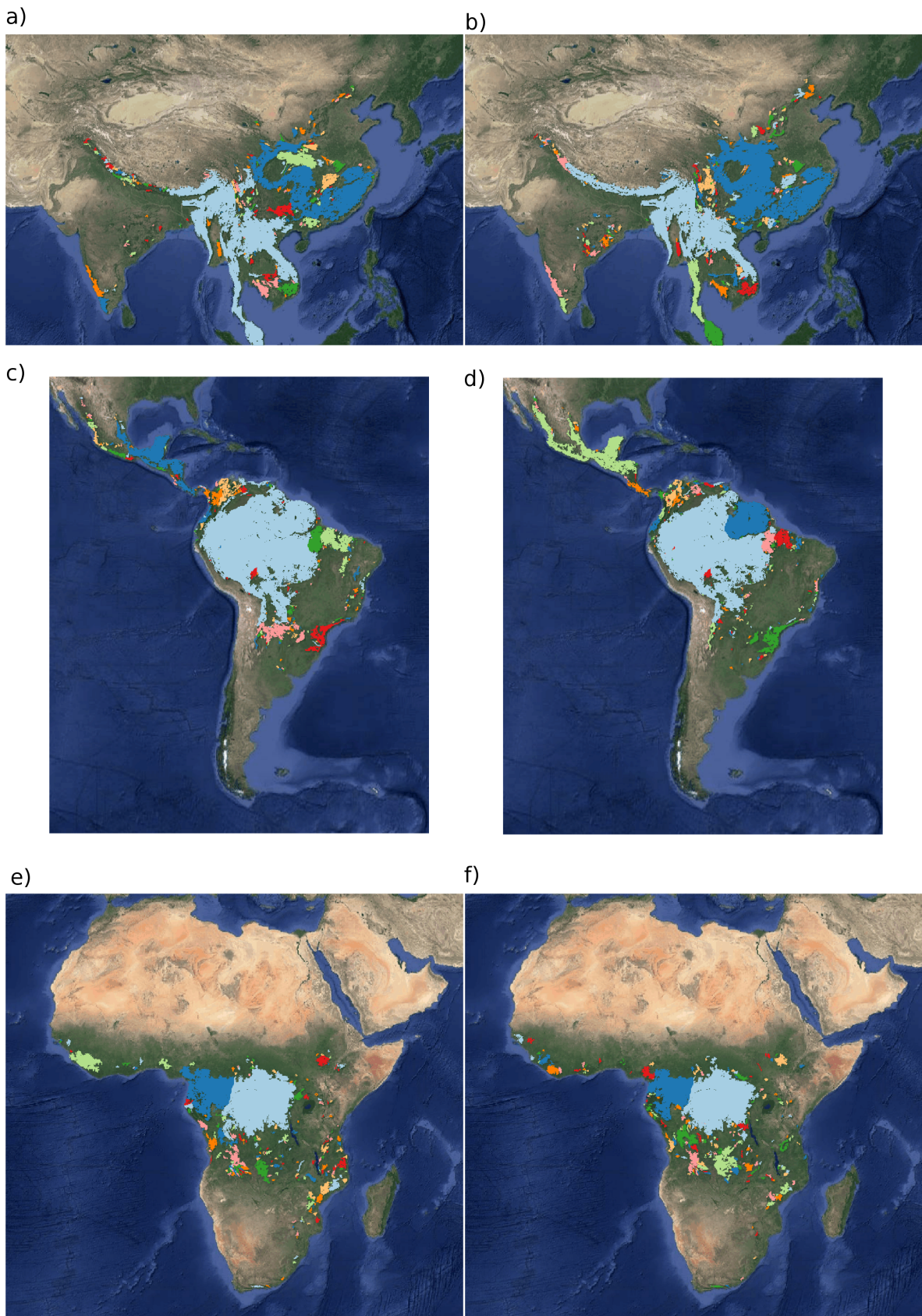


Figure 1: Forest patch distributions for continental regions for the years 2000 and 2014. The images are the 200 biggest patches, showed at a coarse pixel scale of 2.5 Km. The regions are: a) & b) southeast Asia; c) & d) South America subtropical and tropical and e) & f) Africa mainland, for the years 2000 and 2014 respectively.

244 The power law distribution was selected as the best model in 92% of the cases (Appendix S4, Figure S7).
245 In a small number of cases (1%) the power law with exponential cutoff was selected, but the value of the
246 parameter α was similar by ± 0.02 to the pure power law. Additionally the patch size where the exponential
247 tail begins is very large, thus we used the power law parameters for this cases (See Appendix S4, Figure S2,
248 region EUAS3). In finite-size systems the favored model should be the power law with exponential cutoff,
249 because the power-law tails are truncated to the size of the system (Stauffer & Aharony 1994). Here the
250 regions are so large that the cutoff is practically not observed.

251 There is only one region that did not follow a power law: Eurasia mainland, which showed a log-normal
252 distribution, representing 7% of the cases. The log-normal and power law are both heavy tailed distributions
253 and difficult to distinguish, but in this case Akaike weights have very high values for log-normal (near 1),
254 meaning that this is the only possible model. In addition, the goodness of fit tests clearly rejected the power
255 law model in all cases for this region (Appendix S4, table S1, region EUAS1). In general the goodness of fit
256 test rejected the power law model in fewer than 10% of cases. In large forest areas like Africa mainland (AF1)
257 or South America tropical-subtropical (SAST1), larger deviations are expected and the rejections rates are
258 higher so the proportion is 30% or less (Appendix S4, Table S1).

259 Taking into account the bootstrapped confidence intervals of each power law exponent (α) and the temporal
260 autocorrelation, there were no significant differences between α for the regions with the biggest (greater than
261 10^7 km^2) forest areas (Figure 2 and Appendix S4, Figure S8). There were also no differences between these
262 regions and smaller ones (Appendix S4, Tables S2 & S3), and all the slopes of α were not different from
263 0 (Appendix S4, Table S3). This implies a global average $\alpha = 1.908$, with a bootstrapped 95% confidence
264 interval between 1.898 and 1.920.

265 The proportion of the largest patch relative to total forest area RS_{max} for regions with more than 10^7 km^2
266 of forest is shown in figure 3. South America tropical and subtropical (SAST1) and North America (NA1)
267 have a higher RS_{max} of more than 60%, and other big regions 40% or less. For regions with less total
268 forest area (Appendix S4, figure S9 & Table 1), the United Kingdom (EUAS3) has a very low proportion
269 near 1%, while other regions such as New Guinea (OC2) and Malaysia/Kalimantan (OC3) have a very high
270 proportion. SEAS2 (Philippines) is a very interesting case because it seems to be under 30% until the year
271 2005, fluctuates in the range 30-60%, and then stays over 60% (Appendix S4, figure S9).

272 We analyzed the distributions of fluctuations of the largest patch relative to total forest area ΔRS_{max}
273 and the fluctuations of the largest patch ΔS_{max} . The model selection for ΔS_{max} resulted in power law
274 distributions for all regions (Appendix S4, table S6). For ΔRS_{max} instead some regions showed exponential
275 distributions: Eurasia mainland (EUAS1), New Guinea (OC2), Malaysia (OC3), New Zealand (OC6, OC8)

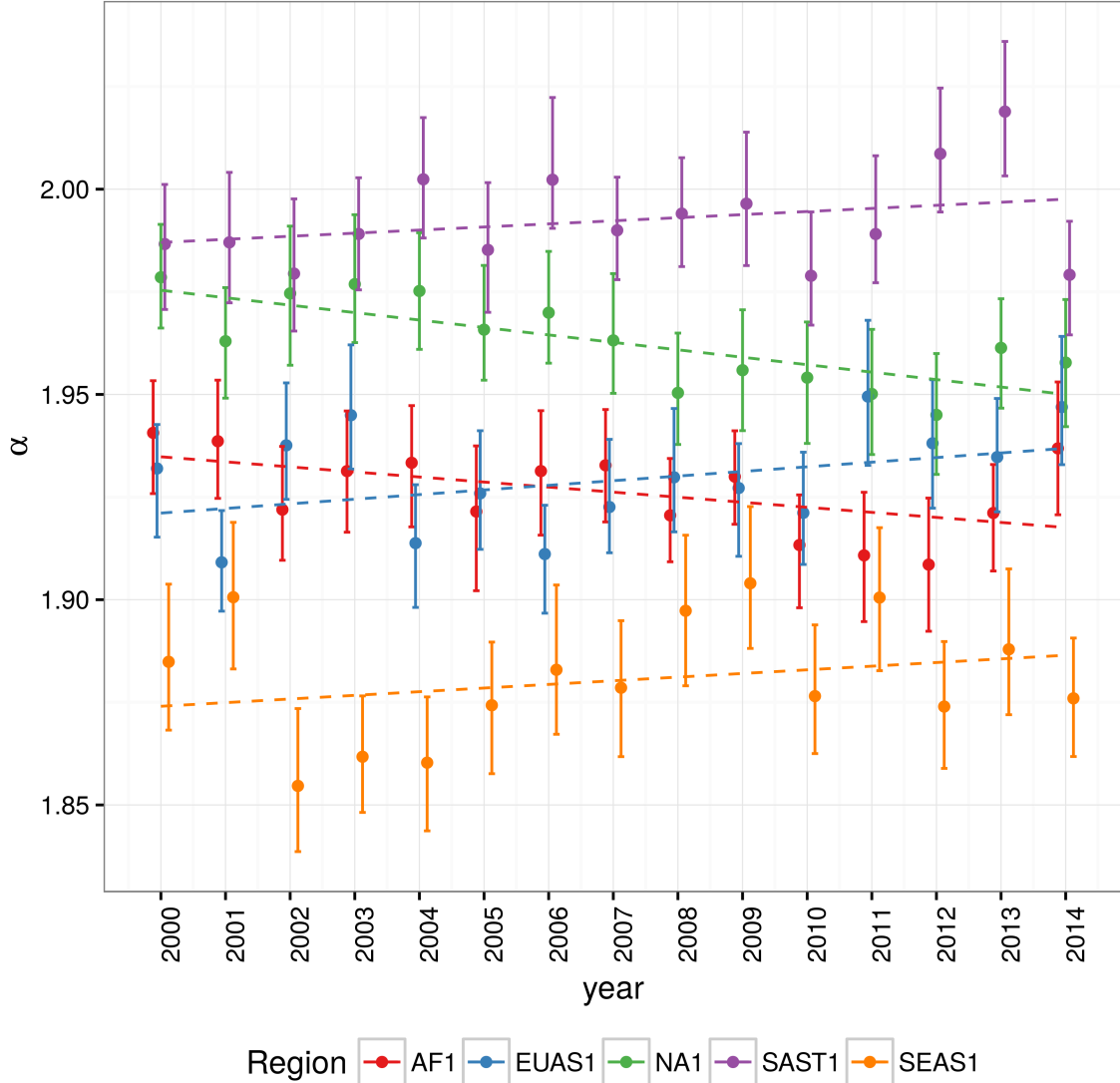


Figure 2: Power law exponents (α) of forest patch distributions for regions with total forest area $> 10^7 \text{ km}^2$. Dashed horizontal lines are the fitted generalized least squares linear model, with 95% confidence interval error bars estimated by bootstrap resampling. The regions are AF1: Africa mainland, EUAS1: Eurasia mainland, NA1: North America mainland, SAST1: South America subtropical and tropical, SEAS1: Southeast Asia mainland. For EUAS1 the best model is log-normal but the exponents are included here for comparison.

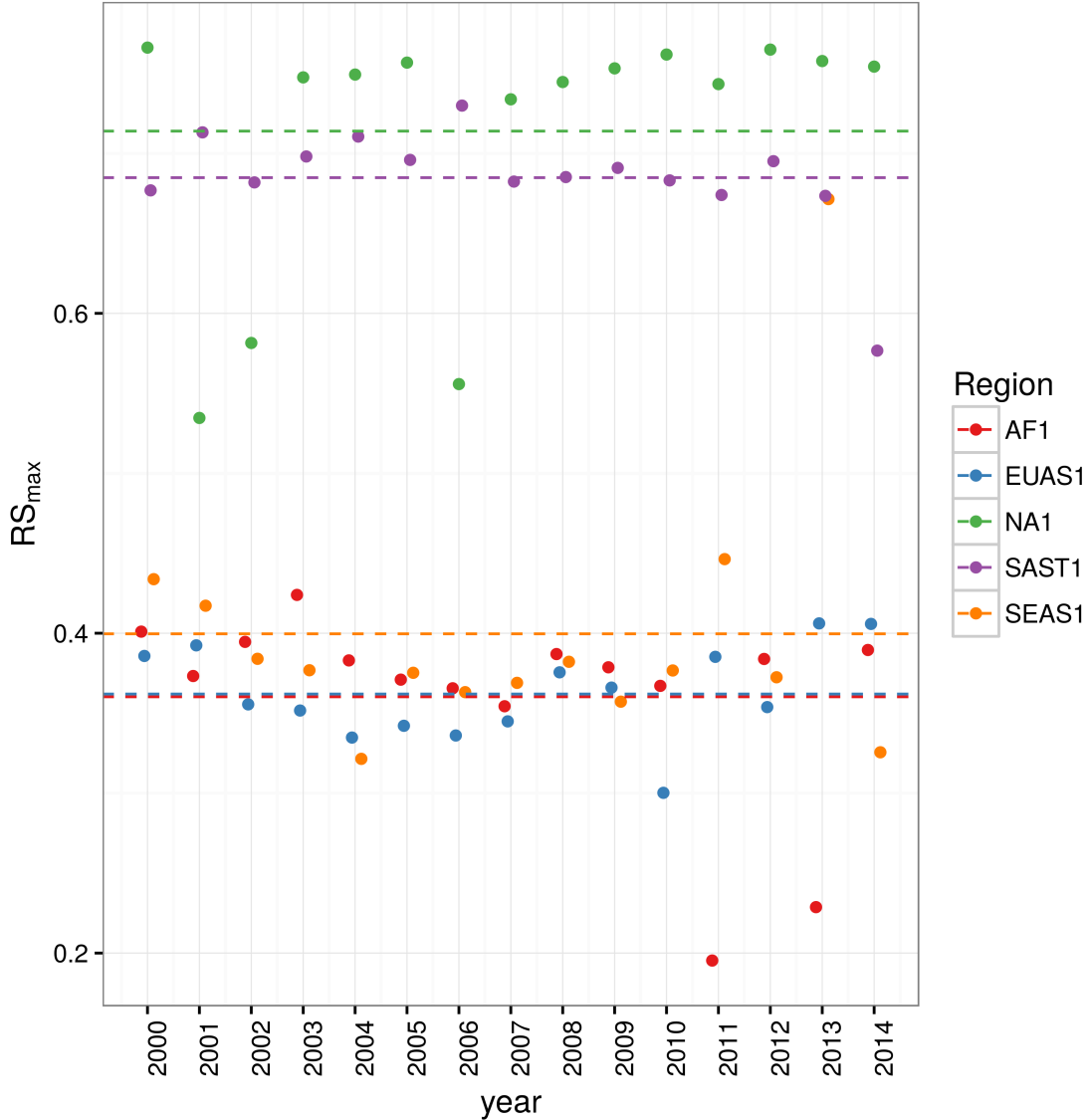


Figure 3: Largest patch proportion relative to total forest area RS_{max} , for regions with total forest area $> 10^7 \text{ km}^2$. Dashed lines are averages across time. The regions are AF1: Africa mainland, EUAS1: Eurasia mainland, NA1: North America mainland, SAST1: South America tropical and subtropical, SEAS1: Southeast Asia mainland.

276 and Java (OC7), all others were power laws (Appendix S4, Table S7). The goodness of fit test (GOF) did
277 not reject power laws in any case, but neither did it reject the other models except in a few cases; this was
278 due to the small number of observations. We only considered fluctuations to follow a power law when this
279 distribution was selected for both absolute and relative fluctuations.

280 The animations of the two largest patches (see supplementary data, largest patch gif animations) qualitatively
281 shows the nature of fluctuations and if the state of the forest is connected or not. If the largest patch is
282 always the same patch over time, the forest is probably not fragmented; this happens for regions with RS_{max}
283 of more than 40% such as AF2 (Madagascar), NA1 (North America), and OC3 (Malaysia). In the regions
284 with RS_{max} between 40% and 30% the identity of the largest patch could change or stay the same in time.
285 For OC7 (Java) the largest patch changes and for AF1 (Africa mainland) it stays the same. Only for EUAS1
286 (Eurasia mainland) we observed that the two largest patches are always the same, implying that this region
287 is probably composed of two independent domains and should be divided in further studies. The regions
288 with RS_{max} less than 25%: SAST2 (Cuba) and EUAS3 (United Kingdom), the largest patch always changes
289 reflecting their fragmented state. In the case of SEAS2 (Philippines) a transition is observed, with the
290 identity of the largest patch first variable, and then constant after 2010.

291 The results of quantile regressions are identical for ΔRS_{max} and ΔS_{max} (Appendix S4, table S4). Among the
292 biggest regions, Africa (AF1) has upper and lower quantiles with significantly negative slopes, but the lower
293 quantile slope is lower, implying that negative fluctuations and variance are increasing (Figure 4). Eurasia
294 mainland (EUAS1) has only the upper quantile significant with a positive slope, suggesting an increase in the
295 variance. North America mainland (NA1) exhibits a significant lower quantile with positive slope, implying
296 decreasing variance. Finally, for mainland Australia, all quantiles are significant, and the slope of the lower
297 quantiles is greater than the upper ones, showing that variance is decreasing (Appendix S4, figure S10).
298 These results are summarized in Table 1.

299 The conditions that indicate that a region is near a critical fragmentation threshold are that patch size
300 distributions follow a power law; temporal ΔRS_{max} fluctuations follow a power law; variance of ΔRS_{max} is
301 increasing in time; and skewness is negative. All these conditions were true only for Africa mainland (AF1)
302 and South America tropical & subtropical (SAST1).

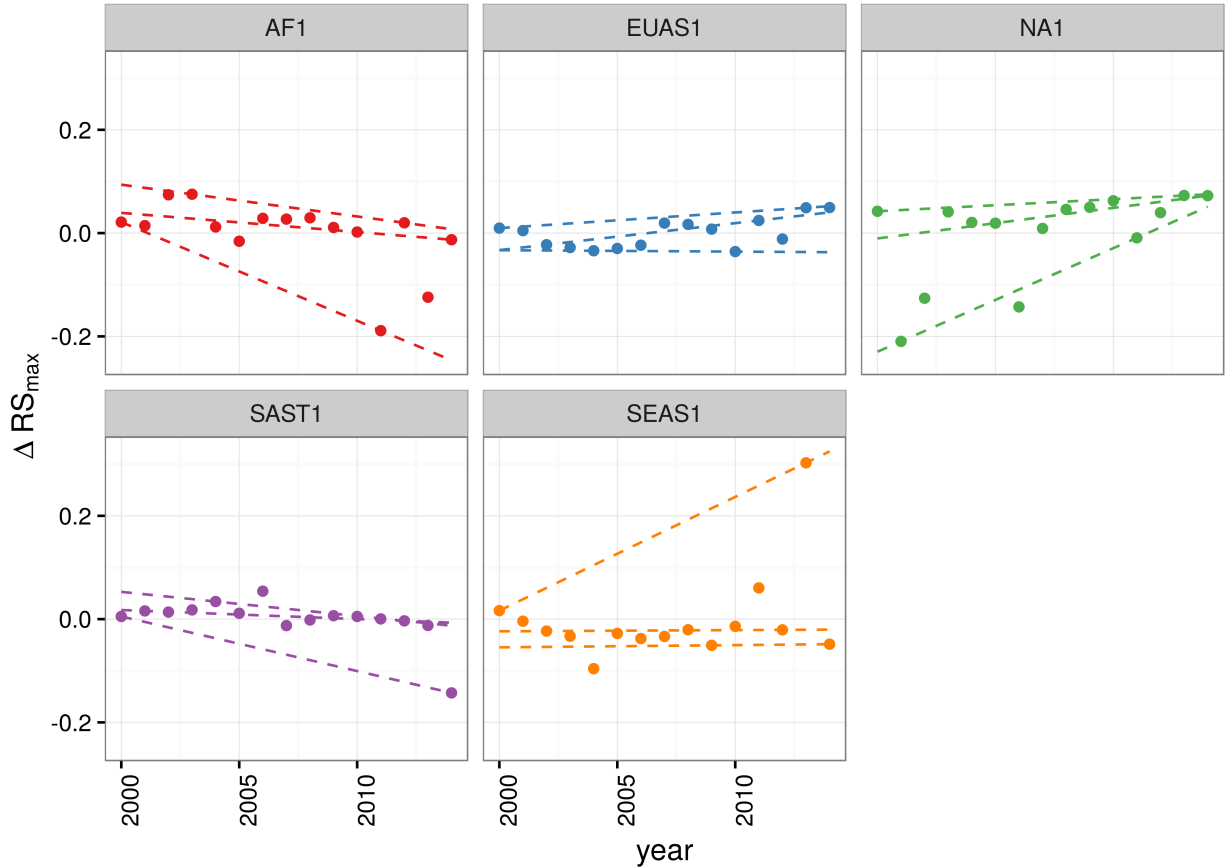


Figure 4: Largest patch fluctuations for regions with total forest area $> 10^7 \text{ km}^2$ across years. The patch sizes are relative to the total forest area of the same year. Dashed lines are 90%, 50% and 10% quantile regressions, to show if fluctuations were increasing. The regions are AF1: Africa mainland, EUAS1: Eurasia mainland, NA1: North America mainland, SAST1: South America tropical and subtropical, SEAS1: Southeast Asia mainland.

Table 1: Regions and indicators of closeness to a critical fragmentation threshold. Where, RS_{max} is the largest patch divided by the total forest area, ΔRS_{max} are the fluctuations of RS_{max} around the mean, skewness was calculated for RS_{max} and the increase or decrease in the variance was estimated using quantile regressions, NS means the results were non-significant. The conditions that determine the closeness to a threshold are: power law distributions in patch sizes and ΔRS_{max} ; increasing variance of ΔRS_{max} and negative skewness.

Region	Description	Average	Patch Size			
		RS_{max}	Distrib	ΔRS_{max}	Distrib.	Skewness
AF1	Africa mainland	0.36	Power	Power	-1.8630	Increase
AF2	Madagascar	0.65	Power	Power	-0.2478	NS
EUAS1	Eurasia, mainland	0.36	LogNormal	Exp	0.4016	Increase
EUAS2	Japan	0.94	Power	Power	0.0255	NS
EUAS3	United Kingdom	0.07	Power	Power	2.1330	NS
NA1	North America, mainland	0.71	Power	Power	-1.5690	Decrease
NA5	Newfoundland	0.87	Power	Power	-0.7411	NS
OC1	Australia, Mainland	0.28	Power	Power	0.0685	Decrease
OC2	New Guinea	0.97	Power	Exp	0.1321	Decrease
OC3	Malaysia/Kalimantan	0.97	Power	Exp	-0.9633	NS
OC4	Sumatra	0.92	Power	Power	1.3150	Increase
OC5	Sulawesi	0.87	Power	Power	-0.3863	NS
OC6	New Zealand South Island	0.76	Power	Exp	-0.6683	NS
OC7	Java	0.38	Power	Exp	-0.1948	NS
OC8	New Zealand North Island	0.75	Power	Exp	0.2940	NS
SAST1	South America, Tropical and subtropical forest up to Mexico	0.68	Power	Power	-2.7760	Increase
SAST2	Cuba	0.21	Power	Power	0.2751	NS
SAT1	South America, Temperate forest	0.60	Power	Power	-1.5070	Decrease
SEAS1	Southeast Asia, Mainland	0.40	Power	Power	3.0030	NS
SEAS2	Philippines	0.54	Power	Power	0.3113	Increase

303 Discussion

304 We found that the forest patch distribution of most regions of the world followed power laws spanning
 305 seven orders of magnitude. These include tropical rainforest, boreal and temperate forest. Power laws have
 306 previously been found for several kinds of vegetation, but never at global scales as in this study. Interestingly,
 307 Eurasia does not follow a power law, but it is a geographically extended region, consisting of different domains
 308 (as we observed in the largest patch animations, see supplementary data). It is known that the union of two
 309 independent power law distributions produces a lognormal distribution (Rooij *et al.* 2013). Future studies
 310 should split this region into two or more new regions, and test if the underlying distributions are power laws.
 311 Several mechanisms have been proposed for the emergence of power laws in forest: the first is related self
 312 organized criticality (SOC), when the system is driven by its internal dynamics to a critical state; this has

been suggested mainly for fire-driven forests (Zinck & Grimm 2009; Hantson, Pueyo & Chuvieco 2015). Real ecosystems do not seem to meet the requirements of SOC dynamics (Sole, Alonso & Mckane 2002; Pueyo *et al.* 2010; McKenzie & Kennedy 2012). A second possible mechanism, suggested by Pueyo *et al.* (2010), is isotropic percolation, when a system is near the critical point power law structures arise. This is equivalent to the random forest model that we explained previously, and requires the tuning of an external environmental condition to carry the system to this point. We did not expect forest growth to be a random process at local scales, but it is possible that combinations of factors cancel out to produce seemingly random forest dynamics at large scales. If this is the case the power law exponent should be theoretically near $\alpha = 2.055$; this is close but outside the confidence interval we observed (1.898 - 1.920). The third mechanism suggested as the cause of pervasive power laws in patch size distribution is facilitation (Manor & Shnerb 2008; Irvine, Bull & Keeling 2016): a patch surrounded by forest will have a smaller probability of been deforested or degraded than an isolated patch. We hypothesize that models that include facilitation could explain the patterns observed here. The model of Scanlon *et al.* (2007) showed an $\alpha = 1.34$ which is also different from our results. Another model but with three states (tree/non-tree/degraded), including local facilitation and grazing, was also used to obtain power laws patch distributions without external tuning, and exhibited deviations from power laws at high grazing pressures (Kéfi *et al.* 2007). The values of the power law exponent α obtained for this model are dependent on the intensity of facilitation, when facilitation is more intense the exponent is higher, but the maximal values they obtained are still lower than the ones we observed. The interesting point is that the value of the exponent is dependent on the parameters, and thus the observed α might be obtained with some parameter combination.

It has been suggested that a combination of spatial and temporal indicators could more reliably detect critical transitions (Kéfi *et al.* 2014). In this study, we combined five criteria to detect the closeness to a fragmentation threshold. Two of them were spatial: the forest patch size distribution, and the proportion of the largest patch relative to total forest area (RS_{max}). The other three were the distribution of temporal fluctuations in the largest patch size, the trend in the variance, and the skewness of the fluctuations. Each one of these is not a strong individual predictor, but their combination gives us an increased degree of confidence about the system being close to a critical transition.

We found that only the tropical forest of Africa and South America met all five criteria, and thus seem to be near a critical fragmentation threshold. This confirms previous studies that point to these two tropical areas as the most affected by deforestation (Hansen *et al.* 2013). Africa seems to be more affected, because the proportion of the largest patch relative to total forest area (RS_{max}) is near 30%, which could indicate that the transition is already started. Moreover, this region was estimated to be potentially bistable, with

345 the possibility to completely transform into a savanna (Staver, Archibald & Levin 2011). The main driver
346 of deforestation in this area was smallholder farming.

347 The region of South America tropical forest has a RS_{max} of more than 60%, suggesting that the fragmentation
348 transition is approaching but not yet started. In this region, a striking decline in deforestation rates has
349 been observed in Brasil, which hosts most of the biggest forest patch, but deforestation rates have continued
350 to increase in surrounding countries (Argentina, Paraguay, Bolivia, Colombia, Peru) thus the region is still
351 at a high risk.

352 The monitoring of biggest patches is also important because they contain most of the intact forest landscapes
353 defined by Potapov *et al.* (2008), thus a relatively simple way to evaluate the risk in these areas is to use
354 RS_{max} index. The analysis of RS_{max} reveals that the island of Philippines (SEAS2) seems to be an example
355 of a critical transition from an unconnected to a connected state, the early warning signals can be qualitatively
356 observed: a big fluctuation in a negative direction precedes the transition and then RS_{max} stabilizes over
357 60% (Figure S9). In addition, there was a total loss of forest cover of 1.9% from year 2000 to 2012 (Hansen *et*
358 *al.* 2013) and deforestation rates were not substantially reduced in 1990-2014; this could be the results of an
359 active intervention of the government promoting conservation and rehabilitation of protected areas, ban of
360 logging old-growth forest, reforestation of barren areas, community-based forestry activities, and sustainable
361 forest management in the country's production forest (Lasco *et al.* 2008). This confirms that the early
362 warning indicators proposed here work in the correct direction.

363 The region of Southeast Asia was also one of the most deforested places in the world, but was not detected
364 as a region near a fragmentation threshold. This is probably due to the forest conservation and restoration
365 programs implemented by the Chinese government, which bans logging in natural forests and monitor illegal
366 harvesting (Viña *et al.* 2016). The MODIS dataset does not detect if native forest is replaced by agroindus-
367 trial tree plantations like oil palms, that are among the main drivers of deforestation in this area (Malhi *et*
368 *al.* 2014). To improve the estimation of forest patches, data sets as the MODIS cropland probability and
369 others about land use, protected areas, forest type, should be incorporated (Hansen *et al.* 2014; Sexton *et*
370 *al.* 2015).

371 Deforestation and fragmentation are closely related. At low levels of habitat reduction species population
372 will decline proportionally; this can happen even when the habitat fragments retain connectivity. As habi-
373 tat reduction continues, the critical threshold is approached and connectivity will have large fluctuations
374 (Brook *et al.* 2013). This could trigger several negative synergistic effects: populations fluctuations and the
375 possibility of extinctions will rise, increasing patch isolation and decreasing connectivity (Brook *et al.* 2013).
376 This positive feedback mechanism will be enhanced when the fragmentation threshold is reached, resulting

377 in the loss of most habitat specialist species at a landscape scale (Pardini *et al.* 2010). Some authors argue
378 that since species have heterogeneous responses to habitat loss and fragmentation, and biotic dispersal is
379 limited, the importance of thresholds is restricted to local scales or even that its existence is questionable
380 (Brook *et al.* 2013). Fragmentation is by definition a local process that at some point produces emergent
381 phenomena over the entire landscape, even if the area considered is infinite (Oborny, Meszéna & Szabó
382 2005). In addition, after a region's fragmentation threshold connectivity decreases, there is still a large and
383 internally well connected patch that can maintain sensitive species (Martensen *et al.* 2012). What is the
384 time needed for these large patches to become fragmented, and pose a real danger of extinction to a myriad
385 of sensitive species? If a forest is already in a fragmented state, a second critical transition from forest to
386 non-forest could happen, this was called the desertification transition (Corrado *et al.* 2014). Considering
387 the actual trends of habitat loss, and studying the dynamics of non-forest patches—instead of the forest
388 patches as we did here—the risk of this kind of transition could be estimated. The simple models proposed
389 previously could also be used to estimate if these thresholds are likely to be continuous and reversible or
390 discontinuous and often irreversible (Weissmann & Shnerb 2016), and the degree of protection (e.g. using
391 the set-asides strategy Banks-Leite *et al.* (2014)) than would be necessary to stop this trend.

392 The effectiveness of landscape management is related to the degree of fragmentation, and the criteria to direct
393 reforestation efforts could be focused on regions near a transition (Oborny *et al.* 2007). Regions that are in
394 an unconnected state require large efforts to recover a connected state, but regions that are near a transition
395 could be easily pushed to a connected state; feedbacks due to facilitation mechanisms might help to maintain
396 this state. Crossing the fragmentation critical point in forests could have negative effects on biodiversity and
397 ecosystem services (Haddad *et al.* 2015), but it could also produce feedback loops at different levels of the
398 biological hierarchy. This means that a critical transition produced at a continental scale could have effects
399 at the level of communities, food webs, populations, phenotypes and genotypes (Barnosky *et al.* 2012). All
400 these effects interact with climate change, thus there is a potential production of cascading effects that could
401 lead to a global collapse. Therefore, even if critical thresholds are reached only in some forest regions at a
402 continental scale, a cascading effect with global consequences could still be produced, and may contribute to
403 reach a planetary tipping point (Reyer *et al.* 2015). The risk of such event will be higher if the dynamics of
404 separate continental regions are coupled (Lenton & Williams 2013). Using the time series obtained in this
405 work the coupling of the continental could be further investigated. It has been proposed that to assess the
406 probability of a global scale shift, different small scale ecosystems should be studied in parallel (Barnosky *et*
407 *al.* 2012). As forest comprises a major proportion of such ecosystems, we think that the transition of forests
408 could be used as a proxy for all the underling changes and as a successful predictor of a planetary tipping

⁴⁰⁹ point.

⁴¹⁰ **Supporting information**

⁴¹¹ **Appendix**

⁴¹² *Table S1:* Proportion of Power law models not rejected by the goodness of fit test at $p \leq 0.05$ level.

⁴¹³ *Table S2:* Generalized least squares fit by maximizing the restricted log-likelihood.

⁴¹⁴ *Table S3:* Simultaneous Tests for General Linear Hypotheses of the power law exponent.

⁴¹⁵ *Table S4:* Quantile regressions of the proportion of largest patch area vs year.

⁴¹⁶ *Table S5:* Unbiased estimation of skewness for absolute largest patch fluctuations and relative fluctuations.

⁴¹⁷ *Table S6:* Model selection using Akaike criterion for largest patch fluctuations in absolute values

⁴¹⁸ *Table S7:* Model selection for fluctuation of largest patch in relative to total forest area.

⁴¹⁹ *Figure S1:* Regions for Africa (AF), 1 Mainland, 2 Madagascar.

⁴²⁰ *Figure S2:* Regions for Eurasia (EUAS), 1 Mainland, 2 Japan, 3 United Kingdom.

⁴²¹ *Figure S3:* Regions for North America (NA), 1 Mainland, 5 Newfoundland.

⁴²² *Figure S4:* Regions for Australia and islands (OC), 1 Australia mainland; 2 New Guinea; 3 Malaysia/Kalimantan;

⁴²³ 4 Sumatra; 5 Sulawesi; 6 New Zealand south island; 7 Java; 8 New Zealand north island.

⁴²⁴ *Figure S5:* Regions for South America, SAST1 Tropical and subtropical forest up to Mexico; SAST2 Cuba;

⁴²⁵ SAT1 South America, Temperate forest.

⁴²⁶ *Figure S6:* Regions for Southeast Asia (SEAS), 1 Mainland; 2 Philippines.

⁴²⁷ *Figure S7:* Proportion of best models selected for patch size distributions using the Akaike criterion.

⁴²⁸ *Figure S8:* Power law exponents for forest patch distributions by year.

⁴²⁹ *Figure S9:* Largest patch proportion relative to total forest area RS_{max} , for regions with total forest area

⁴³⁰ less than 10^7 km^2 .

⁴³¹ *Figure S10:* Fluctuations of largest patch for regions with total forest area less than 10^7 km^2 . The patch

⁴³² sizes are relativized to the total forest area for that year.

433 **Data Accessibility**

434 Csv text file with model fits for patch size distribution, and model selection for all the regions; Gif Animations
435 of a forest model percolation; Gif animations of largest patches; patch size files for all years and regions
436 used here; and all the R and Matlab scripts are available at figshare <http://dx.doi.org/10.6084/m9.figshare.4263905>.

438 **Acknowledgments**

439 LAS and SRD are grateful to the National University of General Sarmiento for financial support. This work
440 was partially supported by a grant from CONICET (PIO 144-20140100035-CO).

441 **References**

- 442 Allington, G.R.H. & Valone, T.J. (2010) Reversal of desertification: The role of physical and chemical soil
443 properties. *Journal of Arid Environments*, **74**, 973–977.
- 444 Banks-Leite, C., Pardini, R., Tambosi, L.R., Pearse, W.D., Bueno, A.A., Bruscagin, R.T., Condez, T.H.,
445 Dixo, M., Igari, A.T., Martensen, A.C. & Metzger, J.P. (2014) Using ecological thresholds to evaluate the
446 costs and benefits of set-asides in a biodiversity hotspot. *Science*, **345**, 1041–1045.
- 447 Barnosky, A.D., Hadly, E.A., Bascompte, J., Berlow, E.L., Brown, J.H., Fortelius, M., Getz, W.M., Harte, J.,
448 Hastings, A., Marquet, P.A., Martinez, N.D., Mooers, A., Roopnarine, P., Vermeij, G., Williams, J.W., Gille-
449 spie, R., Kitzes, J., Marshall, C., Matzke, N., Mindell, D.P., Revilla, E. & Smith, A.B. (2012) Approaching
450 a state shift in Earth’s biosphere. *Nature*, **486**, 52–58.
- 451 Bascompte, J. & Solé, R.V. (1996) Habitat fragmentation and extinction thresholds in spatially explicit
452 models. *Journal of Animal Ecology*, **65**, 465–473.
- 453 Bazant, M.Z. (2000) Largest cluster in subcritical percolation. *Physical Review E*, **62**, 1660–1669.
- 454 Belward, A.S. (1996) *The IGBP-DIS Global 1 Km Land Cover Data Set “DISCover”: Proposal and Imple-
455 mentation Plans : Report of the Land Recover Working Group of IGBP-DIS*. IGBP-DIS Office.
- 456 Benedetti-Cecchi, L., Tamburello, L., Maggi, E. & Bulleri, F. (2015) Experimental Perturbations Modify the
457 Performance of Early Warning Indicators of Regime Shift. *Current biology*, **25**, 1867–1872.
- 458 Bestelmeyer, B.T., Ellison, A.M., Fraser, W.R., Gorman, K.B., Holbrook, S.J., Laney, C.M., Ohman, M.D.,

- 459 Peters, D.P.C., Pillsbury, F.C., Rassweiler, A., Schmitt, R.J. & Sharma, S. (2011) Analysis of abrupt tran-
460 sitions in ecological systems. *Ecosphere*, **2**, 129.
- 461 Boettiger, C. & Hastings, A. (2012) Quantifying limits to detection of early warning for critical transitions.
462 *Journal of The Royal Society Interface*, **9**, 2527–2539.
- 463 Bonan, G.B. (2008) Forests and Climate Change: forcings, Feedbacks, and the Climate Benefits of Forests.
464 *Science*, **320**, 1444–1449.
- 465 Botet, R. & Ploszajczak, M. (2004) Correlations in Finite Systems and Their Universal Scaling Properties.
466 *Nonequilibrium physics at short time scales: Formation of correlations* (ed K. Morawetz), pp. 445–466.
467 Springer-Verlag, Berlin Heidelberg.
- 468 Brook, B.W., Ellis, E.C., Perring, M.P., Mackay, A.W. & Blomqvist, L. (2013) Does the terrestrial biosphere
469 have planetary tipping points? *Trends in Ecology & Evolution*.
- 470 Burnham, K. & Anderson, D.R. (2002) *Model selection and multi-model inference: A practical information-*
471 *theoretic approach*, 2nd. ed. Springer-Verlag, New York.
- 472 Canfield, D.E., Glazer, A.N. & Falkowski, P.G. (2010) The Evolution and Future of Earth's Nitrogen Cycle.
473 *Science*, **330**, 192–196.
- 474 Carpenter, S.R., Cole, J.J., Pace, M.L., Batt, R., Brock, W.A., Cline, T., Coloso, J., Hodgson, J.R., Kitchell,
475 J.F., Seekell, D.A., Smith, L. & Weidel, B. (2011) Early Warnings of Regime Shifts: A Whole-Ecosystem
476 Experiment. *Science*, **332**, 1079–1082.
- 477 Clauset, A., Shalizi, C. & Newman, M. (2009) Power-Law Distributions in Empirical Data. *SIAM Review*,
478 **51**, 661–703.
- 479 Corrado, R., Cherubini, A.M. & Pennetta, C. (2014) Early warning signals of desertification transitions in
480 semiarid ecosystems. *Physical Review E - Statistical, Nonlinear, and Soft Matter Physics*, **90**, 62705.
- 481 Crowther, T.W., Glick, H.B., Covey, K.R., Bettigole, C., Maynard, D.S., Thomas, S.M., Smith, J.R., Hintler,
482 G., Duguid, M.C., Amatulli, G., Tuanmu, M.-N., Jetz, W., Salas, C., Stam, C., Piotto, D., Tavani, R., Green,
483 S., Bruce, G., Williams, S.J., Wiser, S.K., Huber, M.O., Hengeveld, G.M., Nabuurs, G.-J., Tikhonova, E.,
484 Borchardt, P., Li, C.-F., Powrie, L.W., Fischer, M., Hemp, A., Homeier, J., Cho, P., Vibrans, A.C., Umunay,
485 P.M., Piao, S.L., Rowe, C.W., Ashton, M.S., Crane, P.R. & Bradford, M.A. (2015) Mapping tree density at
486 a global scale. *Nature*, **525**, 201–205.
- 487 Dai, L., Vorselen, D., Korolev, K.S. & Gore, J. (2012) Generic Indicators for Loss of Resilience Before a

- 488 Tipping Point Leading to Population Collapse. *Science*, **336**, 1175–1177.
- 489 DiMiceli, C., Carroll, M., Sohlberg, R., Huang, C., Hansen, M. & Townshend, J. (2015) Annual Global
490 Automated MODIS Vegetation Continuous Fields (MOD44B) at 250 m Spatial Resolution for Data Years
491 Beginning Day 65, 2000 - 2014, Collection 051 Percent Tree Cover, University of Maryland, College Park,
492 MD, USA.
- 493 Drake, J.M. & Griffen, B.D. (2010) Early warning signals of extinction in deteriorating environments. *Nature*,
494 **467**, 456–459.
- 495 Efron, B. & Tibshirani, R.J. (1994) *An Introduction to the Bootstrap*. Taylor & Francis, New York.
- 496 Filotas, E., Parrott, L., Burton, P.J., Chazdon, R.L., Coates, K.D., Coll, L., Haeussler, S., Martin, K.,
497 Nocentini, S., Puettmann, K.J., Putz, F.E., Simard, S.W. & Messier, C. (2014) Viewing forests through the
498 lens of complex systems science. *Ecosphere*, **5**, 1–23.
- 499 Foley, J.A., Ramankutty, N., Brauman, K.A., Cassidy, E.S., Gerber, J.S., Johnston, M., Mueller, N.D.,
500 O’Connell, C., Ray, D.K., West, P.C., Balzer, C., Bennett, E.M., Carpenter, S.R., Hill, J., Monfreda, C.,
501 Polasky, S., Rockström, J., Sheehan, J., Siebert, S., Tilman, D. & Zaks, D.P.M. (2011) Solutions for a
502 cultivated planet. *Nature*, **478**, 337–342.
- 503 Folke, C., Jansson, Å., Rockström, J., Olsson, P., Carpenter, S.R., Iii, F.S.C., Crépin, A.-S., Daily, G.,
504 Danell, K., Ebbesson, J., Elmquist, T., Galaz, V., Moberg, F., Nilsson, M., Österblom, H., Ostrom, E.,
505 Persson, Å., Peterson, G., Polasky, S., Steffen, W., Walker, B. & Westley, F. (2011) Reconnecting to the
506 Biosphere. *AMBIO*, **40**, 719–738.
- 507 Fung, T., O’Dwyer, J.P., Rahman, K.A., Fletcher, C.D. & Chisholm, R.A. (2016) Reproducing static and
508 dynamic biodiversity patterns in tropical forests: the critical role of environmental variance. *Ecology*, **97**,
509 1207–1217.
- 510 Gardner, R.H. & Urban, D.L. (2007) Neutral models for testing landscape hypotheses. *Landscape Ecology*,
511 **22**, 15–29.
- 512 Gastner, M.T., Oborny, B., Zimmermann, D.K. & Pruessner, G. (2009) Transition from Connected to Frag-
513 mented Vegetation across an Environmental Gradient: Scaling Laws in Ecotone Geometry. *The American
514 Naturalist*, **174**, E23–E39.
- 515 Gillespie, C.S. (2015) Fitting Heavy Tailed Distributions: The poweRlaw Package. *Journal of Statistical
516 Software*, **64**, 1–16.
- 517 Gilman, S.E., Urban, M.C., Tewksbury, J., Gilchrist, G.W. & Holt, R.D. (2010) A framework for community

- 518 interactions under climate change. *Trends in Ecology & Evolution*, **25**, 325–331.
- 519 Goldstein, M.L., Morris, S.A. & Yen, G.G. (2004) Problems with fitting to the power-law distribution. *The*
520 *European Physical Journal B - Condensed Matter and Complex Systems*, **41**, 255–258.
- 521 Haddad, N.M., Brudvig, L.a., Clobert, J., Davies, K.F., Gonzalez, A., Holt, R.D., Lovejoy, T.E., Sexton,
522 J.O., Austin, M.P., Collins, C.D., Cook, W.M., Damschen, E.I., Ewers, R.M., Foster, B.L., Jenkins, C.N.,
523 King, a.J., Laurance, W.F., Levey, D.J., Margules, C.R., Melbourne, B.a., Nicholls, a.O., Orrock, J.L.,
524 Song, D.-X. & Townshend, J.R. (2015) Habitat fragmentation and its lasting impact on Earth's ecosystems.
525 *Science Advances*, **1**, 1–9.
- 526 Hansen, M., Potapov, P., Margono, B., Stehman, S., Turubanova, S. & Tyukavina, A. (2014) Response to
527 Comment on “High-resolution global maps of 21st-century forest cover change”. *Science*, **344**, 981.
- 528 Hansen, M.C., Potapov, P.V., Moore, R., Hancher, M., Turubanova, S.A., Tyukavina, A., Thau, D., Stehman,
529 S.V., Goetz, S.J., Loveland, T.R., Kommareddy, A., Egorov, A., Chini, L., Justice, C.O. & Townshend, J.R.G.
530 (2013) High-Resolution Global Maps of 21st-Century Forest Cover Change. *Science*, **342**, 850–853.
- 531 Hantson, S., Pueyo, S. & Chuvieco, E. (2015) Global fire size distribution is driven by human impact and
532 climate. *Global Ecology and Biogeography*, **24**, 77–86.
- 533 Harris, T.E. (1974) Contact interactions on a lattice. *The Annals of Probability*, **2**, 969–988.
- 534 Hastings, A. & Wysham, D.B. (2010) Regime shifts in ecological systems can occur with no warning. *Ecology*
535 *Letters*, **13**, 464–472.
- 536 He, F. & Hubbell, S. (2003) Percolation Theory for the Distribution and Abundance of Species. *Physical*
537 *Review Letters*, **91**, 198103.
- 538 Hinrichsen, H. (2000) Non-equilibrium critical phenomena and phase transitions into absorbing states. *Ad-*
539 *vances in Physics*, **49**, 815–958.
- 540 Irvine, M.A., Bull, J.C. & Keeling, M.J. (2016) Aggregation dynamics explain vegetation patch-size distri-
541 butions. *Theoretical Population Biology*, **108**, 70–74.
- 542 Keitt, T.H., Urban, D.L. & Milne, B.T. (1997) Detecting critical scales in fragmented landscapes. *Conser-*
543 *vation Ecology*, **1**, 4.
- 544 Kéfi, S., Guttal, V., Brock, W.A., Carpenter, S.R., Ellison, A.M., Livina, V.N., Seekell, D.A., Scheffer, M.,
545 Nes, E.H. van & Dakos, V. (2014) Early Warning Signals of Ecological Transitions: Methods for Spatial

- 546 Patterns. *PLoS ONE*, **9**, e92097.
- 547 Kéfi, S., Rietkerk, M., Alados, C.L., Pueyo, Y., Papanastasis, V.P., ElAich, A. & Ruiter, P.C. de. (2007)
- 548 Spatial vegetation patterns and imminent desertification in Mediterranean arid ecosystems. *Nature*, **449**,
- 549 213–217.
- 550 Kitzberger, T., Aráoz, E., Gowda, J.H., Mermoz, M. & Morales, J.M. (2012) Decreases in Fire Spread Prob-
- 551 ability with Forest Age Promotes Alternative Community States, Reduced Resilience to Climate Variability
- 552 and Large Fire Regime Shifts. *Ecosystems*, **15**, 97–112.
- 553 Klaus, A., Yu, S. & Plenz, D. (2011) Statistical analyses support power law distributions found in neuronal
- 554 avalanches. (ed M Zochowski). *PloS one*, **6**, e19779.
- 555 Koenker, R. (2016) quantreg: Quantile Regression.
- 556 Lasco, R.D., Pulhin, F.B., Cruz, R.V.O., Pulhin, J.M., Roy, S.S.N. & Sanchez, P.A.J. (2008) Forest responses
- 557 to changing rainfall in the Philippines. *Climate change and vulnerability* (eds N. Leary, C. Conde & J.
- 558 Kulkarni), pp. 49–66. Earthscan, London.
- 559 Leibold, M.A. & Norberg, J. (2004) Biodiversity in metacommunities: Plankton as complex adaptive sys-
- 560 tems? *Limnology and Oceanography*, **49**, 1278–1289.
- 561 Lenton, T.M. & Williams, H.T.P. (2013) On the origin of planetary-scale tipping points. *Trends in Ecology*
- 562 & Evolution, **28**, 380–382.
- 563 Loehle, C., Li, B.-L. & Sundell, R.C. (1996) Forest spread and phase transitions at forest-prairie ecotones in
- 564 Kansas, U.S.A. *Landscape Ecology*, **11**, 225–235.
- 565 Malhi, Y., Gardner, T.A., Goldsmith, G.R., Silman, M.R. & Zelazowski, P. (2014) Tropical Forests in the
- 566 Anthropocene. *Annual Review of Environment and Resources*, **39**, 125–159.
- 567 Manor, A. & Shnerb, N.M. (2008) Origin of pareto-like spatial distributions in ecosystems. *Physical Review*
- 568 *Letters*, **101**, 268104.
- 569 Martensen, A.C., Ribeiro, M.C., Banks-Leite, C., Prado, P.I. & Metzger, J.P. (2012) Associations of Forest
- 570 Cover, Fragment Area, and Connectivity with Neotropical Understory Bird Species Richness and Abundance.
- 571 *Conservation Biology*, **26**, 1100–1111.
- 572 Martín, P.V., Bonachela, J.A., Levin, S.A. & Muñoz, M.A. (2015) Eluding catastrophic shifts. *Proceedings*
- 573 *of the National Academy of Sciences*, **112**, E1828–E1836.
- 574 McKenzie, D. & Kennedy, M.C. (2012) Power laws reveal phase transitions in landscape controls of fire

- 575 regimes. *Nat Commun*, **3**, 726.
- 576 Mitchell, M.G.E., Suarez-Castro, A.F., Martinez-Harms, M., Maron, M., McAlpine, C., Gaston, K.J., Jo-
577 hansen, K. & Rhodes, J.R. (2015) Reframing landscape fragmentation's effects on ecosystem services. *Trends
578 in Ecology & Evolution*, **30**, 190–198.
- 579 Naito, A.T. & Cairns, D.M. (2015) Patterns of shrub expansion in Alaskan arctic river corridors suggest
580 phase transition. *Ecology and Evolution*, **5**, 87–101.
- 581 Oborny, B., Meszéna, G. & Szabó, G. (2005) Dynamics of Populations on the Verge of Extinction. *Oikos*,
582 **109**, 291–296.
- 583 Oborny, B., Szabó, G. & Meszéna, G. (2007) Survival of species in patchy landscapes: percolation in space
584 and time. *Scaling biodiversity*, pp. 409–440. Cambridge University Press.
- 585 Ochoa-Quintero, J.M., Gardner, T.A., Rosa, I., de Barros Ferraz, S.F. & Sutherland, W.J. (2015) Thresholds
586 of species loss in Amazonian deforestation frontier landscapes. *Conservation Biology*, **29**, 440–451.
- 587 Ódor, G. (2004) Universality classes in nonequilibrium lattice systems. *Reviews of Modern Physics*, **76**,
588 663–724.
- 589 Pardini, R., Bueno, A. de A., Gardner, T.A., Prado, P.I. & Metzger, J.P. (2010) Beyond the Fragmentation
590 Threshold Hypothesis: Regime Shifts in Biodiversity Across Fragmented Landscapes. *PLoS ONE*, **5**, e13666.
- 591 Pinheiro, J., Bates, D., DebRoy, S., Sarkar, D. & R Core Team. (2016) *nlme: Linear and Nonlinear Mixed
592 Effects Models*.
- 593 Potapov, P., Yaroshenko, A., Turubanova, S., Dubinin, M., Laestadius, L., Thies, C., Aksenov, D., Egorov,
594 A., Yesipova, Y., Glushkov, I., Karpachevskiy, M., Kostikova, A., Manisha, A., Tsibikova, E. & Zhuravleva,
595 I. (2008) Mapping the world's intact forest landscapes by remote sensing. *Ecology and Society*, **13**.
- 596 Pueyo, S., de Alencastro Graça, P.M.L., Barbosa, R.I., Cots, R., Cardona, E. & Fearnside, P.M. (2010)
597 Testing for criticality in ecosystem dynamics: the case of Amazonian rainforest and savanna fire. *Ecology
598 Letters*, **13**, 793–802.
- 599 R Core Team. (2015) R: A Language and Environment for Statistical Computing.
- 600 Reyer, C.P.O., Rammig, A., Brouwers, N. & Langerwisch, F. (2015) Forest resilience, tipping points and
601 global change processes. *Journal of Ecology*, **103**, 1–4.
- 602 Rockstrom, J., Steffen, W., Noone, K., Persson, A., Chapin, F.S., Lambin, E.F., Lenton, T.M., Scheffer, M.,
603 Folke, C., Schellnhuber, H.J., Nykvist, B., Wit, C.A. de, Hughes, T., Leeuw, S. van der, Rodhe, H., Sorlin,

- 604 S., Snyder, P.K., Costanza, R., Svedin, U., Falkenmark, M., Karlberg, L., Corell, R.W., Fabry, V.J., Hansen,
605 J., Walker, B., Liverman, D., Richardson, K., Crutzen, P. & Foley, J.A. (2009) A safe operating space for
606 humanity. *Nature*, **461**, 472–475.
- 607 Rooij, M.M.J.W. van, Nash, B., Rajaraman, S. & Holden, J.G. (2013) A Fractal Approach to Dynamic
608 Inference and Distribution Analysis. *Frontiers in Physiology*, **4**.
- 609 Saravia, L.A. & Momo, F.R. (2017) Biodiversity collapse and early warning indicators in a spatial phase
610 transition between neutral and niche communities. *PeerJ PrePrints*, **5**, e1589v4.
- 611 Scanlon, T.M., Caylor, K.K., Levin, S.A. & Rodriguez-iturbe, I. (2007) Positive feedbacks promote power-law
612 clustering of Kalahari vegetation. *Nature*, **449**, 209–212.
- 613 Scheffer, M., Bascompte, J., Brock, W.A., Brovkin, V., Carpenter, S.R., Dakos, V., Held, H., Nes, E.H.V.,
614 Rietkerk, M. & Sugihara, G. (2009) Early-warning signals for critical transitions. *Nature*, **461**, 53–59.
- 615 Scheffer, M., Walker, B., Carpenter, S., Foley, J. a, Folke, C. & Walker, B. (2001) Catastrophic shifts in
616 ecosystems. *Nature*, **413**, 591–596.
- 617 Seidler, T.G. & Plotkin, J.B. (2006) Seed Dispersal and Spatial Pattern in Tropical Trees. *PLoS Biology*, **4**,
618 e344.
- 619 Sexton, J.O., Noojipady, P., Song, X.-P., Feng, M., Song, D.-X., Kim, D.-H., Anand, A., Huang, C., Channan,
620 S., Pimm, S.L. & Townshend, J.R. (2015) Conservation policy and the measurement of forests. *Nature*
621 *Climate Change*, **6**, 192–196.
- 622 Sole, R.V., Alonso, D. & Mckane, A. (2002) Self-organized instability in complex ecosystems. *Philosophical
623 transactions of the Royal Society of London. Series B, Biological sciences*, **357**, 667–681.
- 624 Solé, R.V. (2011) *Phase Transitions*. Princeton University Press.
- 625 Solé, R.V. & Bascompte, J. (2006) *Self-organization in complex ecosystems*. Princeton University Press, New
626 Jersey, USA.
- 627 Solé, R.V., Alonso, D. & Saldaña, J. (2004) Habitat fragmentation and biodiversity collapse in neutral
628 communities. *Ecological Complexity*, **1**, 65–75.
- 629 Solé, R.V., Bartumeus, F. & Gamarra, J.G.P. (2005) Gap percolation in rainforests. *Oikos*, **110**, 177–185.
- 630 Stauffer, D. & Aharony, A. (1994) *Introduction To Percolation Theory*. Taylor & Francis, London.
- 631 Staver, A.C., Archibald, S. & Levin, S.A. (2011) The Global Extent and Determinants of Savanna and Forest

- 632 as Alternative Biome States. *Science*, **334**, 230–232.
- 633 Vasilakopoulos, P. & Marshall, C.T. (2015) Resilience and tipping points of an exploited fish population over
634 six decades. *Global Change Biology*, **21**, 1834–1847.
- 635 Viña, A., McConnell, W.J., Yang, H., Xu, Z. & Liu, J. (2016) Effects of conservation policy on China's forest
636 recovery. *Science Advances*, **2**, e1500965.
- 637 Weerman, E.J., Van Belzen, J., Rietkerk, M., Temmerman, S., Kéfi, S., Herman, P.M.J. & Koppell, J.V.
638 de. (2012) Changes in diatom patch-size distribution and degradation in a spatially self-organized intertidal
639 mudflat ecosystem. *Ecology*, **93**, 608–618.
- 640 Weissmann, H. & Shnerb, N.M. (2016) Predicting catastrophic shifts. *Journal of Theoretical Biology*, **397**,
641 128–134.
- 642 Zhang, J.Y., Wang, Y., Zhao, X., Xie, G. & Zhang, T. (2005) Grassland recovery by protection from grazing
643 in a semi-arid sandy region of northern China. *New Zealand Journal of Agricultural Research*, **48**, 277–284.
- 644 Zinck, R.D. & Grimm, V. (2009) Unifying wildfire models from ecology and statistical physics. *The American
645 naturalist*, **174**, E170–85.
- 646 Zuur, A.F., Ieno, E.N., Walker, N., Saveliev, A.A. & Smith, G.M. (2009) *Mixed effects models and extensions
647 in ecology with R*. Springer New York, New York, NY.